Assessing MAGIS capabilities to measure the properties of GW signals from compact binaries

210X.XXXXX w/ Zach Bogorad & Peter W Graham

Sebastian Baum

Stanford University

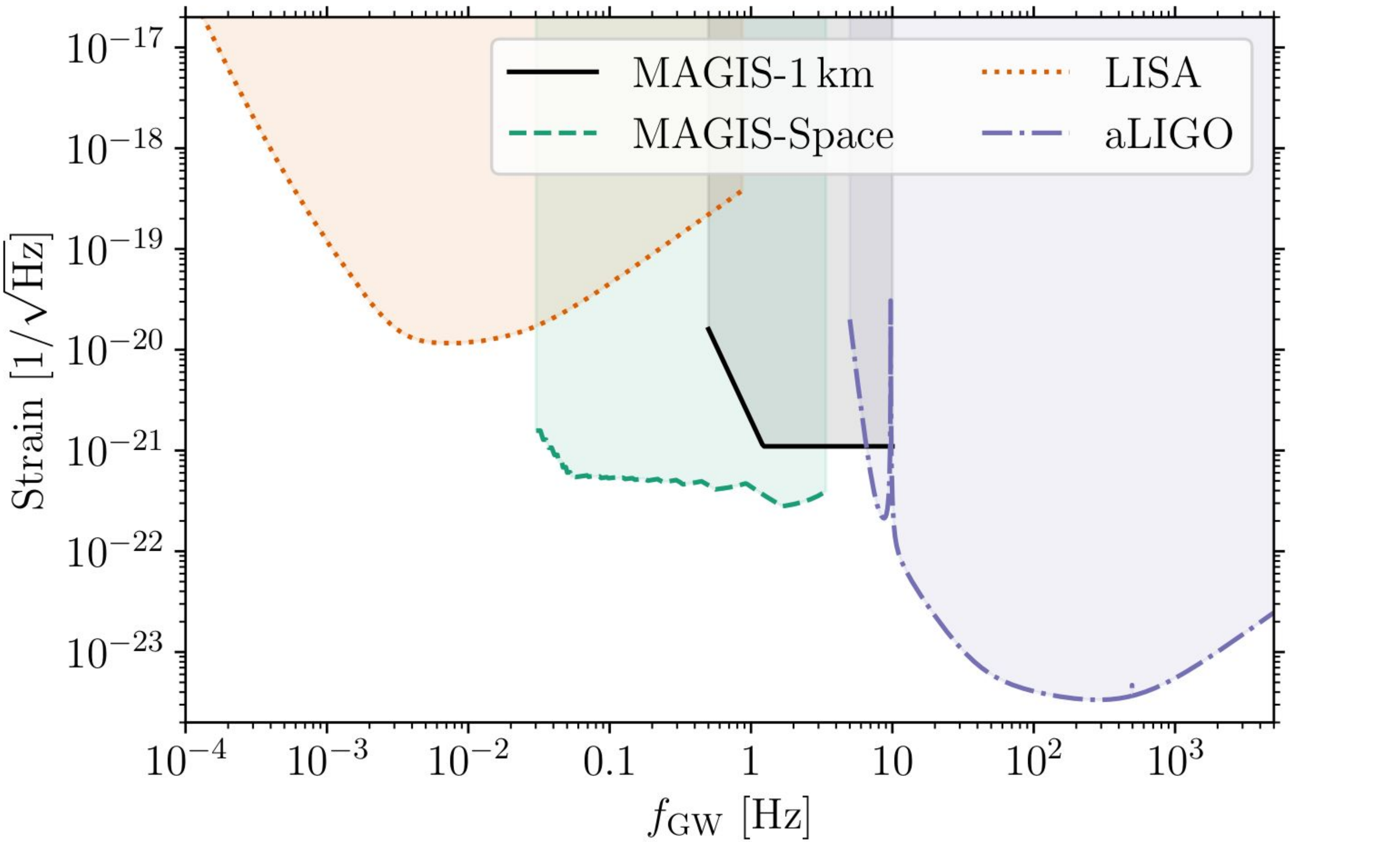
MAGIS-1 km
MAGIS-Space
LISA
aLIGO
Strain $[1/\sqrt{\mathrm{Hz}}]$
10^{-17}
10^{-18}
10^{-19}
10^{-20}
10^{-21}
10^{-22}
10^{-23}
10^{-4}
10^{-3}
10^{-2}
0.1
1
10
10^{2}
10^{3}
f_{GW} [Hz]

1 yr before merger

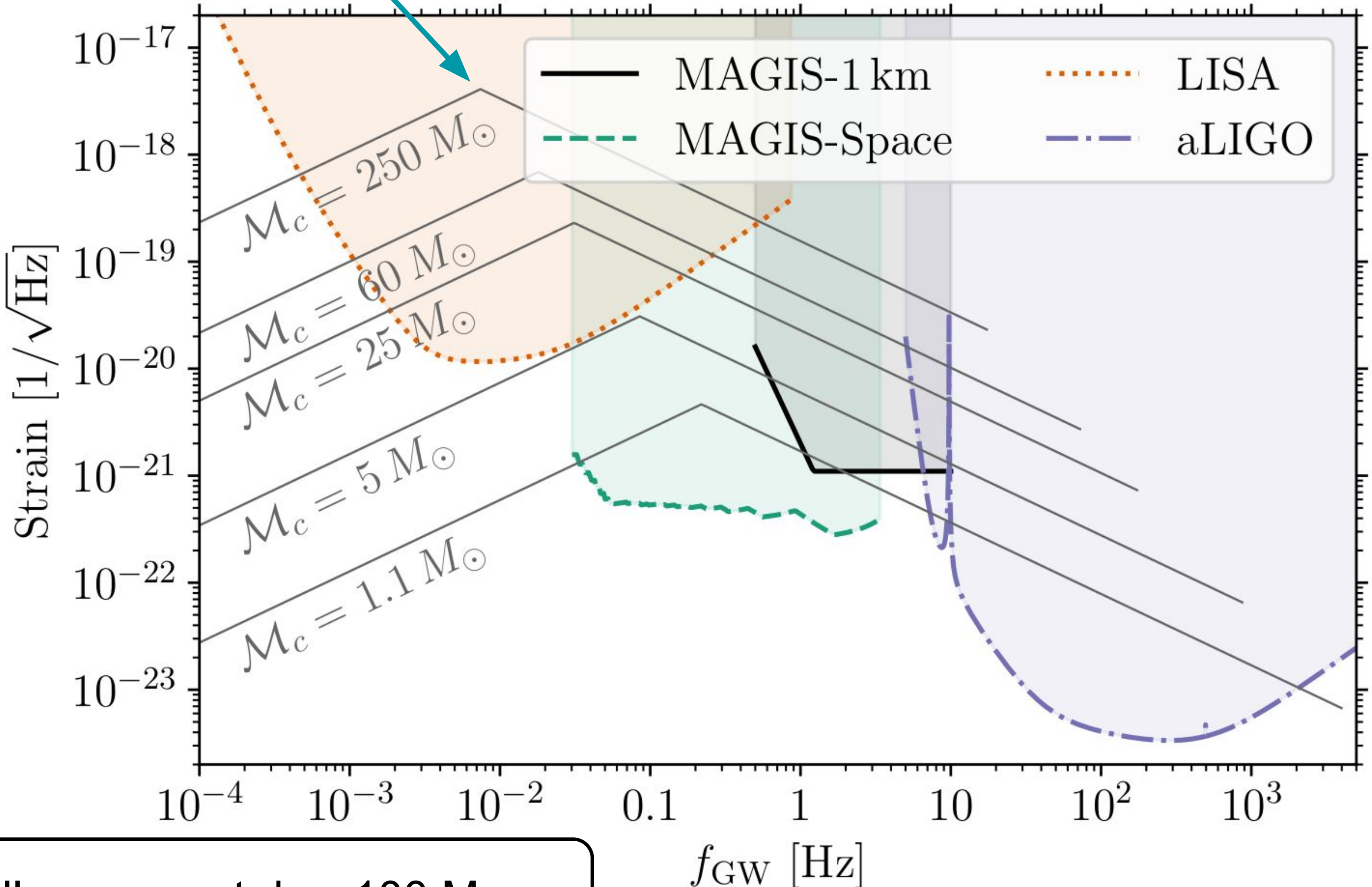

All sources at d_L = 100 Mpc

What is special about AI GW detectors?

- Single baseline

  ⇒ different antenna functions
- Two timescales (atom free-fall time, laser travel time)

  ⇒ different shape of the sensitivity curve
- Terrestrial or mid-Earth orbit

  ⇒ detector re-orientation on hour-timescales
- Small ratio of GW frequency^{-1}/GW wavelength to effective "baseline"

  ⇒ excellent sky localization of sources

Quick reminder of sky-localization capabilities

Three options:

- High signal-to-noise ratio measurement of the waveform in many spatial directions (very hard)
- Time-of-flight between multiple detectors
- Accelerated motion of detector wrt the GW source

Quick reminder of sky-localization capabilities

Three options:

- High signal-to-noise ratio measurement of the waveform in many spatial directions (very hard)
- Time-of-flight between multiple detectors
- Accelerated motion of detector wrt the GW source

Ultimately, these both lead to the diffraction limit:

$$\sigma_{\sqrt{\Omega}} \propto \lambda_{\mathrm{GW}} / L_{\mathrm{baseline}}$$

Quick reminder of sky-localization capabilities

Three options:

- High signal-to-noise ratio measurement of the waveform in many spatial directions (very hard)
- Time-of-flight between multiple detectors
- Accelerated motion of detector wrt the GW source

Ultimately, these both lead to the diffraction limit:

$$\sigma_{\sqrt{\Omega}} \propto \lambda_{\mathrm{GW}} / L_{\mathrm{baseline}}$$

$$\sigma_\Omega^{\mathrm{LIGO}} \sim 10^\circ \left(\frac{1\,\mathrm{kHz}}{f_{\mathrm{GW}}}\right) \quad ; \quad \sigma_\Omega^{\mathrm{AI}} \sim 0.3^\circ \left(\frac{1\,\mathrm{Hz}}{f_{\mathrm{GW}}}\right) \quad ; \quad \sigma_\Omega^{\mathrm{LISA}} \sim 30^\circ \left(\frac{10\,\mathrm{mHz}}{f_{\mathrm{GW}}}\right)$$

Leading-order inspiral waveforms (pol. basis)

- Frequency evolution ("chirp") $$\frac{df_{\mathrm{GW}}}{dt} = \frac{96}{5}\pi^{8/3}\mathcal{M}_c f_{\mathrm{GW}}^{11/3}$$

  with the (detector frame) "chirp mass" $$\mathcal{M}_c = \frac{(m_1 m_2)^{3/5}}{(m_1+m_2)^{1/5}}$$

- Polarization basis waveforms: $\underline{\underline{\boldsymbol{h}}}(t) = h_+(t)\underline{\underline{\boldsymbol{e}}}_+ + h_\times(t)\underline{\underline{\boldsymbol{e}}}_\times$

$$h_{+/\times}(t) = \frac{2\mathcal{M}_c^{5/3}\left[\pi f_{\mathrm{GW}}(t)\right]^{2/3}}{d_L}\begin{cases}\left[1+\left(\hat{\boldsymbol{L}}\cdot\hat{\boldsymbol{n}}\right)^2\right]\cos\Phi_{\mathrm{GW}}(t)\\ 2\left(\hat{\boldsymbol{L}}\cdot\hat{\boldsymbol{n}}\right)\sin\Phi_{\mathrm{GW}}`(t)\end{cases}$$

$$\boxed{\cos\iota \equiv \hat{\boldsymbol{L}}\cdot\hat{\boldsymbol{n}}}$$

Leading-order inspiral waveforms (antenna func.)

- The response of a single-baseline detector is then

$$h(t) = \hat{\boldsymbol{l}}(t)\underline{\underline{\boldsymbol{h}}}(t)\hat{\boldsymbol{l}}(t) = F_+(t)h_+(t) + F_\times(t)h_\times(t)$$

$$\boxed{F_{+/\times}(t) \equiv \hat{\boldsymbol{l}}(t) \cdot \underline{\underline{\boldsymbol{e}}}_{+/\times} \cdot \hat{\boldsymbol{l}}(t)}$$

Parameters describing the binary

Parameter		Benchmark value
Chirp Mass	$\mathcal{M}_c = (m_1 m_2)^{3/5}/(m_1+m_2)^{1/5}$	
Mass ratio	$q = m_1/m_2$	1.15
Luminosity distance	d_L	
Binary phase at $f_{\rm GW}^{\rm ref}$	Φ_0	0
Time of merger	t_c	solar equinox
Inclination angle	ι	45°
Polarization angle	ψ	60°
Right ascension	α	60°
Declination	δ	6.6° (30° above ecliptic)

Overview of the code

Fisher-matrix approach to forecast parameter reconstruction

- Computationally “cheap”
- Only reliable in high signal-to-noise ratio limit

Fisher-matrix approach

- The detector records a time-domain signal: $h(t)$

Fisher-matrix approach

- The detector records a time-domain signal: $h(t)$
- Fourier-transform into the frequency domain,

$$\widetilde{h}(f) = \int_{-\infty}^{\infty} dt\, e^{2\pi i f t} h(t)$$

Fisher-matrix approach

- The detector records a time-domain signal: $h(t)$
- Fourier-transform into the frequency domain,

$$\widetilde{h}(f) = \int_{-\infty}^{\infty} dt \, e^{2\pi i f t} h(t)$$

- Define the inner product: $\langle h, g \rangle = 4 \, \mathrm{Re} \left[\int_0^{\infty} df \, \frac{\widetilde{h}^*(f) \widetilde{g}(f)}{S_n(f)} \right]$

one-sided detector noise PSD

Fisher-matrix approach

- The detector records a time-domain signal: $h(t)$
- Fourier-transform into the frequency domain,

$$\widetilde{h}(f) = \int_{-\infty}^{\infty} dt\, e^{2\pi i f t} h(t)$$

- Define the inner product: $\langle h, g \rangle = 4\,\mathrm{Re}\left[\int_0^{\infty} df\, \frac{\widetilde{h}^*(f)\widetilde{g}(f)}{S_n(f)}\right]$
- Signal-to-noise ratio $\rho^2 = \langle h, h \rangle$

  and Fisher information matrix $\Gamma_{ij} = \left\langle \frac{\partial h}{\partial \theta_i}, \frac{\partial h}{\partial \theta_j} \right\rangle$

Overview of the code

Fisher-matrix approach to forecast parameter reconstruction

- Computationally “cheap”
- Only reliable in high signal-to-noise ratio limit $\mathcal{C}_{ij} = \Gamma^{-1}_{ij}$

Overview of the code

Fisher-matrix approach to forecast parameter reconstruction

- Computationally "cheap"
- Only reliable in high signal-to-noise ratio limit $\mathcal{C}_{ij} = \Gamma^{-1}_{ij}$

- Calculate (3.5/3.0 PN) waveforms in time-domain (good for accelerated det., but computationally expensive)
- FFT to frequency domain (requires choosing window functions… current implementation uses Planck window)
- Some subtleties due to the accelerated detector frame (what do we mean by "detector frame" masses? What is the clock? …)
- Include priors on periodic parameters (α, δ, ι, ψ)

Detector benchmarks

- (Network of) terrestrial MAGIS-1 km detectors

Detector benchmarks

- (Network of) terrestrial MAGIS-1 km detectors

- MAGIS-space in mid-Earth orbit
  - 20,000 km radius / 7.8 h period orbit
  - 3,600 km separation between the satellites
  - Consider orbits inclined {0°, 45°, 90°} to ecliptic
  - For comparison, study also heliocentric orbits at {0.5, 1, 2} AU

Results: SNR in $\mathcal{M}_c - d_L$ plane

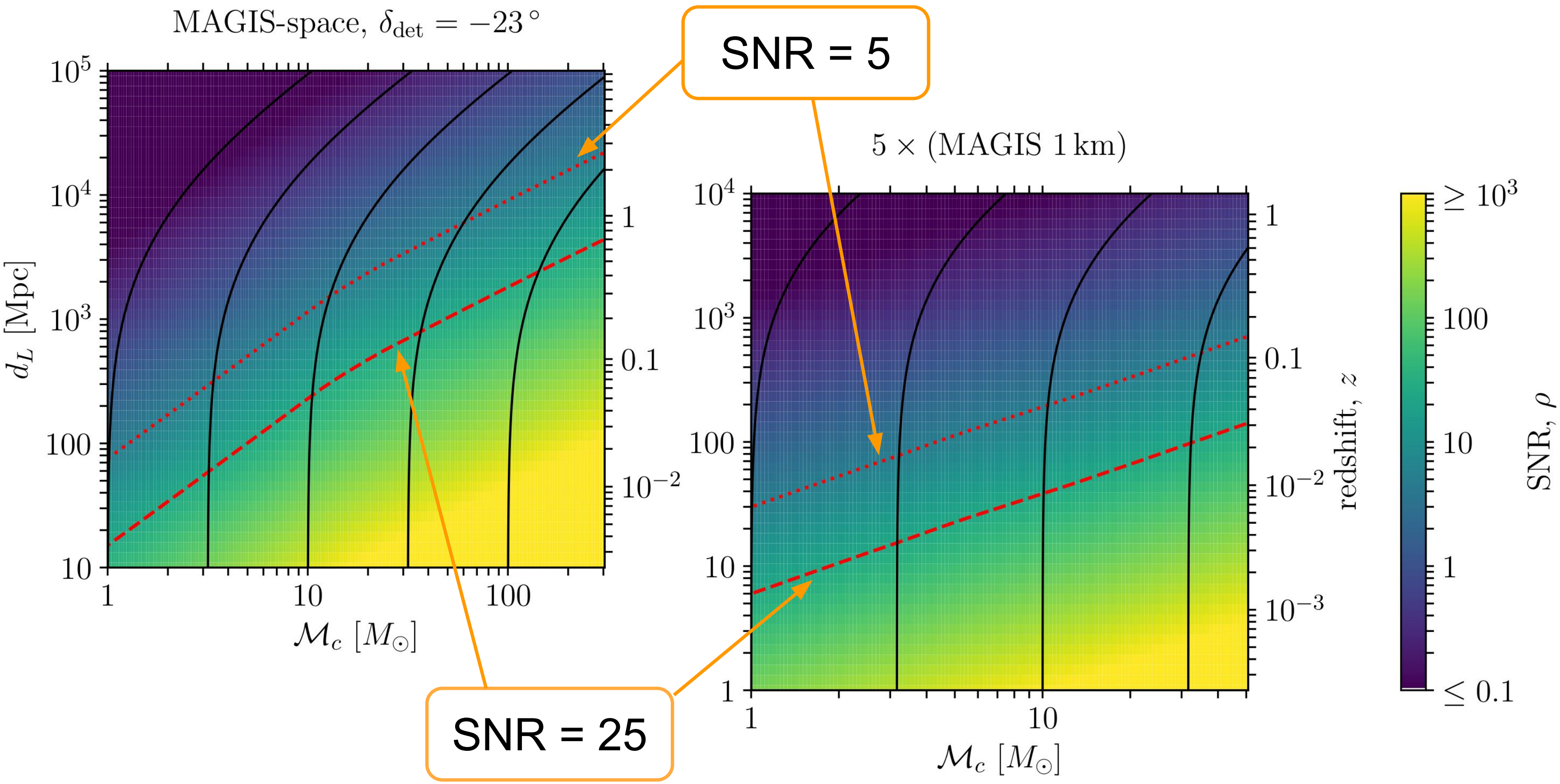

Note different ranges of axes

Heuristics of parameter reconstruction

frequency-evolution (easy)

sub-leading frequency-evolution (~easy)

amplitude (at best 1/SNR)

h_+ vs $h_\times$ amplitude

rotation of e_+ into $e_\times$ in plane ⊥ to $\boldsymbol{n}$

change in Doppler shift

Parameter	
Chirp Mass	$\mathcal{M}_c = (m_1 m_2)^{3/5}/(m_1 + m_2)$
Mass ratio	$q = m_1/m_2$
Luminosity distance	d_L
Binary phase at $f_{\rm GW}^{\rm ref}$	Φ_0
Time of merger	t_c
Inclination angle	ι
Polarization angle	ψ
Right ascension	α
Declination	δ

Results: $\sigma(d_L)$ in $\mathcal{M}_c - d_L$ plane

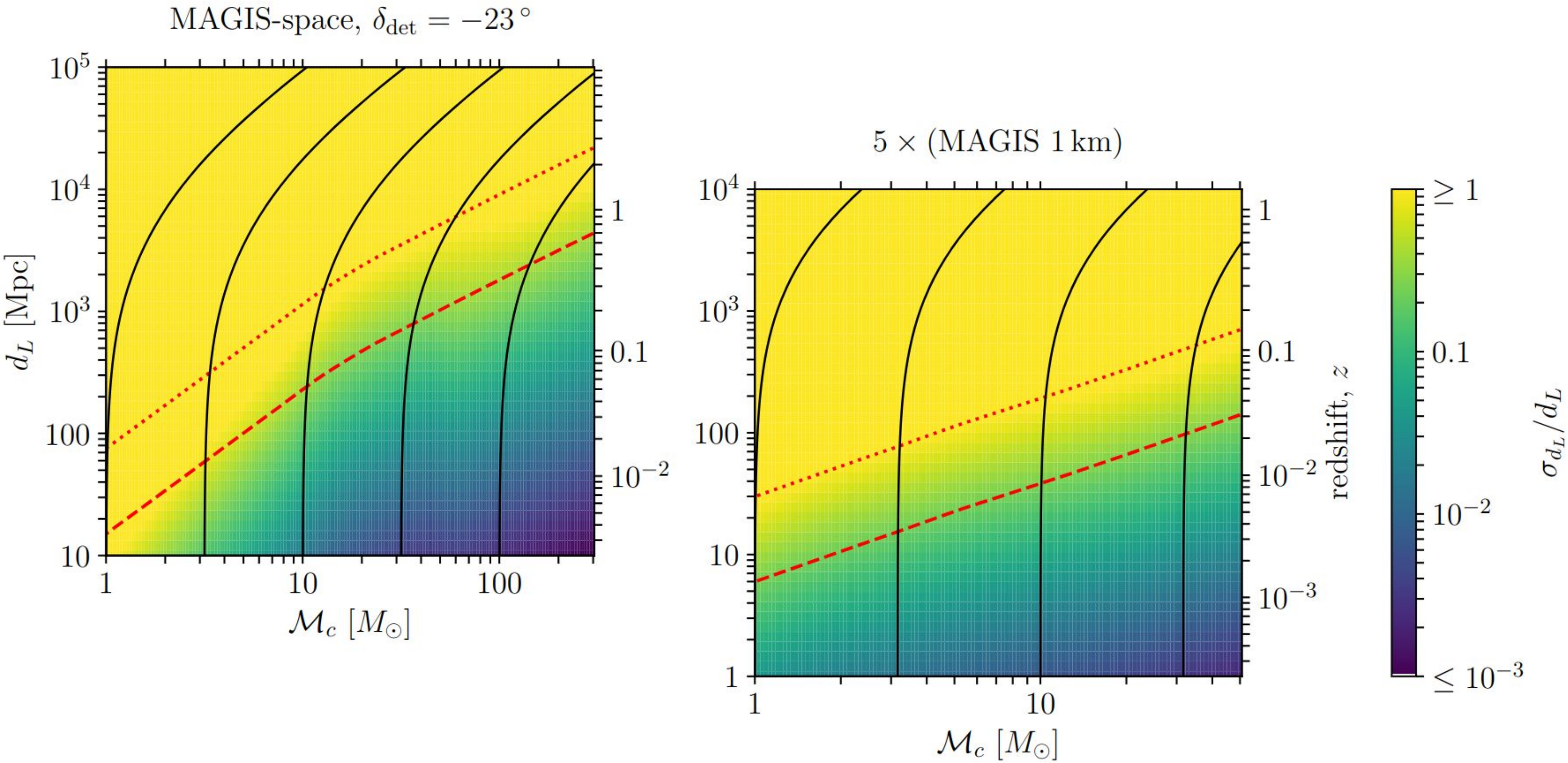

Note different ranges of axes

Results: $\sigma(\sqrt{\Omega_n})$ in $\mathcal{M}_c - d_L$ plane

$$\sigma_{\Omega_n} = 2\pi \cos\delta \sqrt{\mathcal{C}_{\alpha\alpha}\mathcal{C}_{\delta\delta} - \mathcal{C}_{\alpha\delta}^2}$$

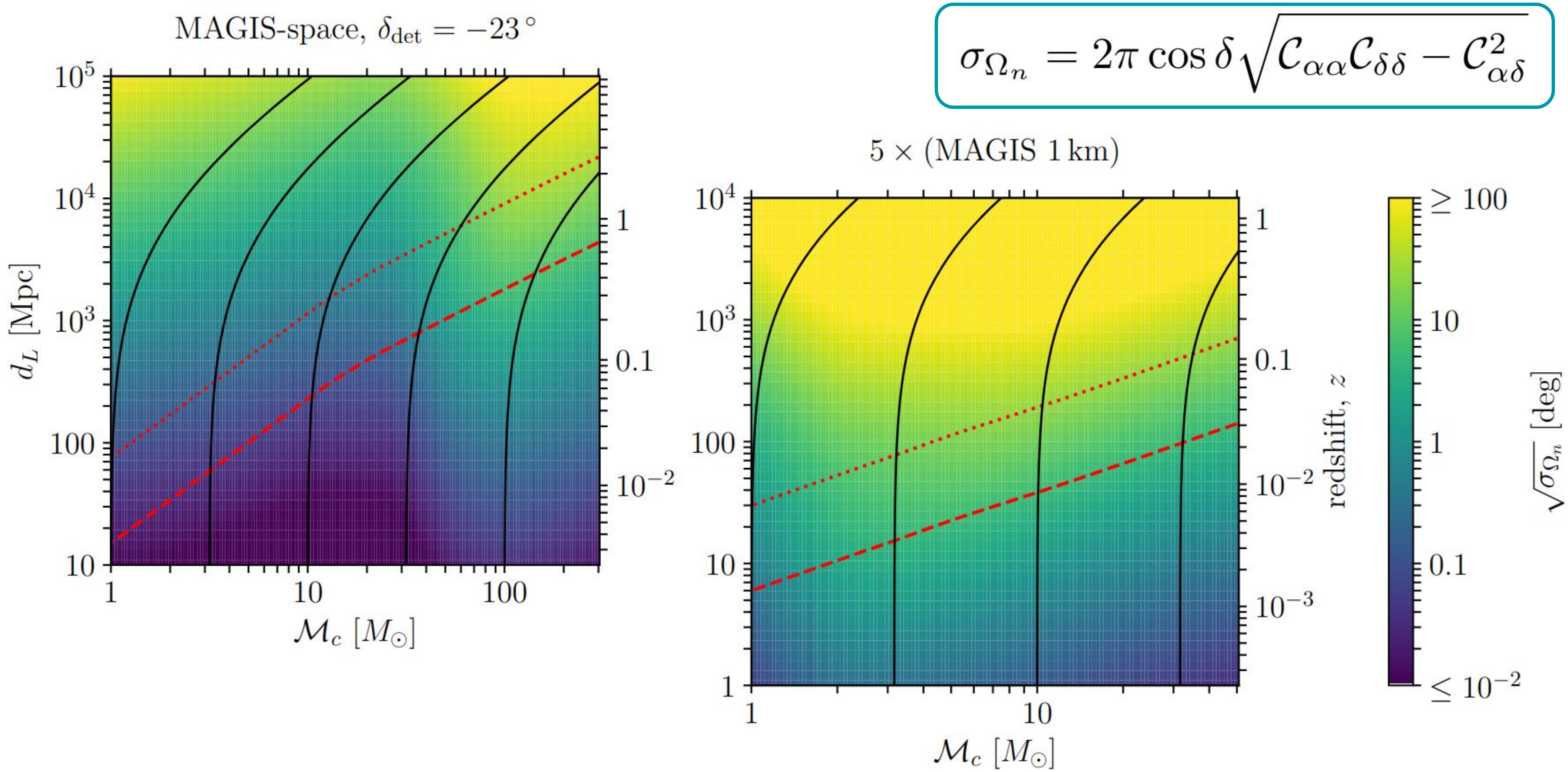

Note different ranges of axes

Terrestrial detectors. SNR in skymap

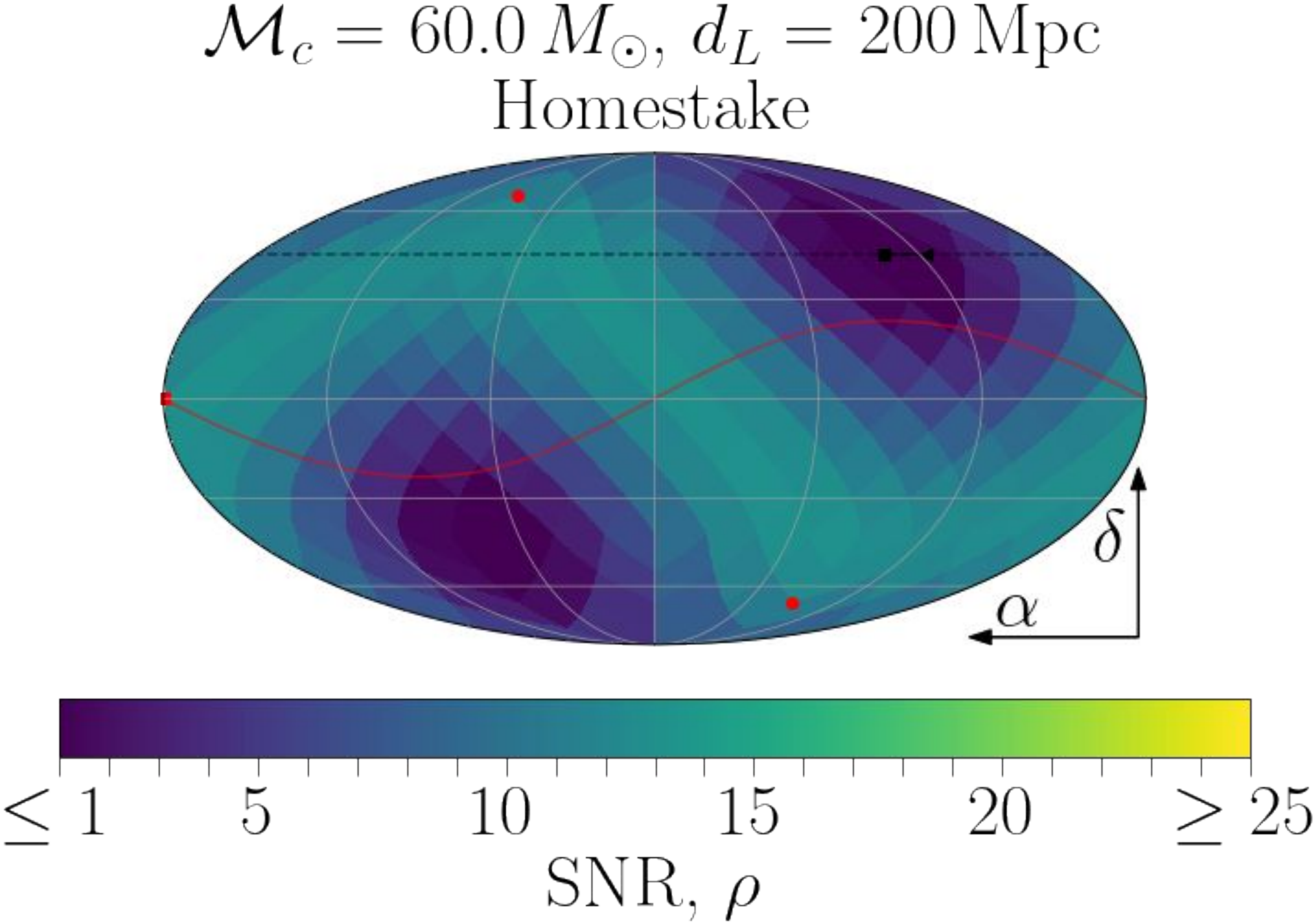

Terrestrial detectors. SNR in skymap

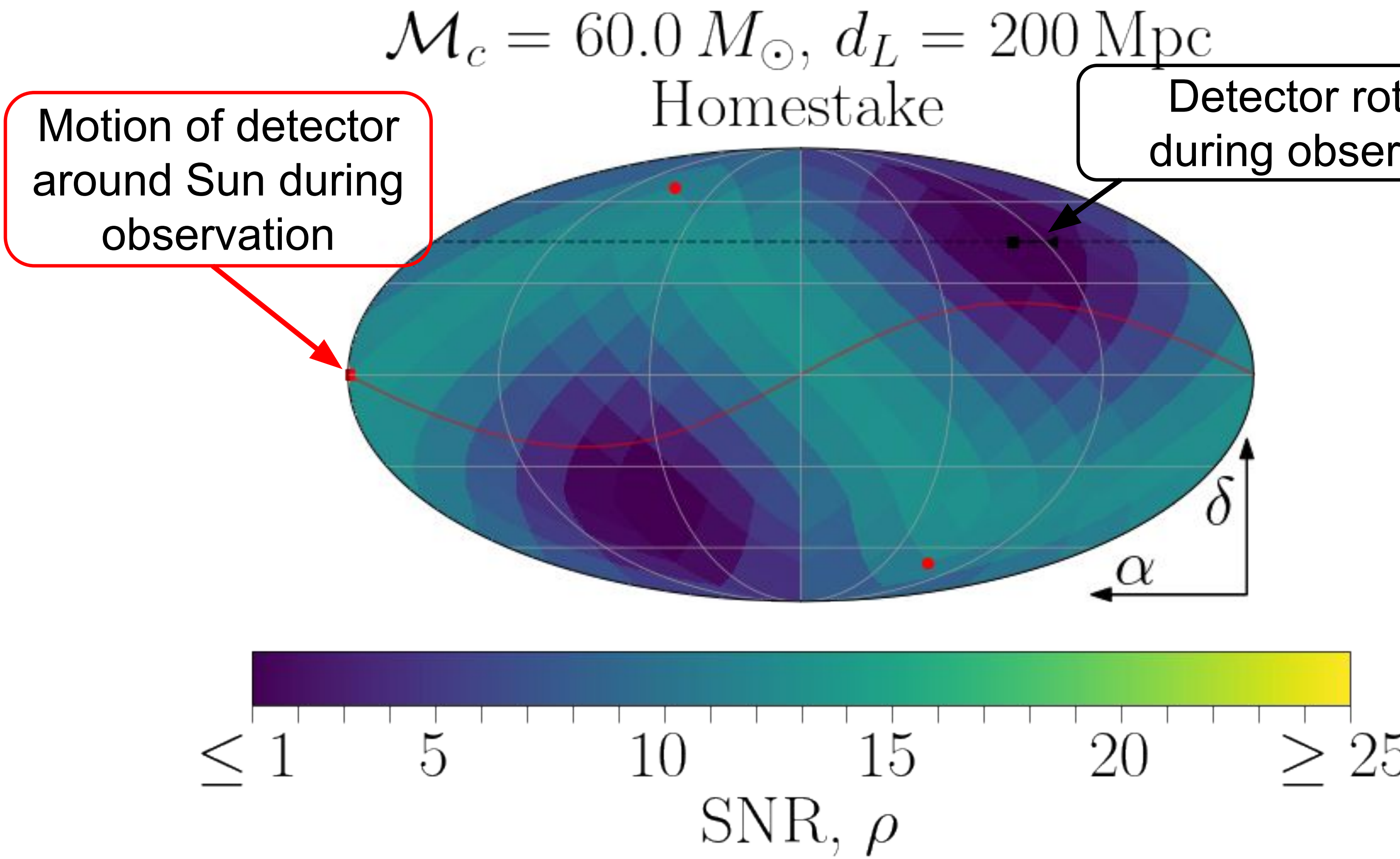

Terrestrial detectors. SNR in skymap

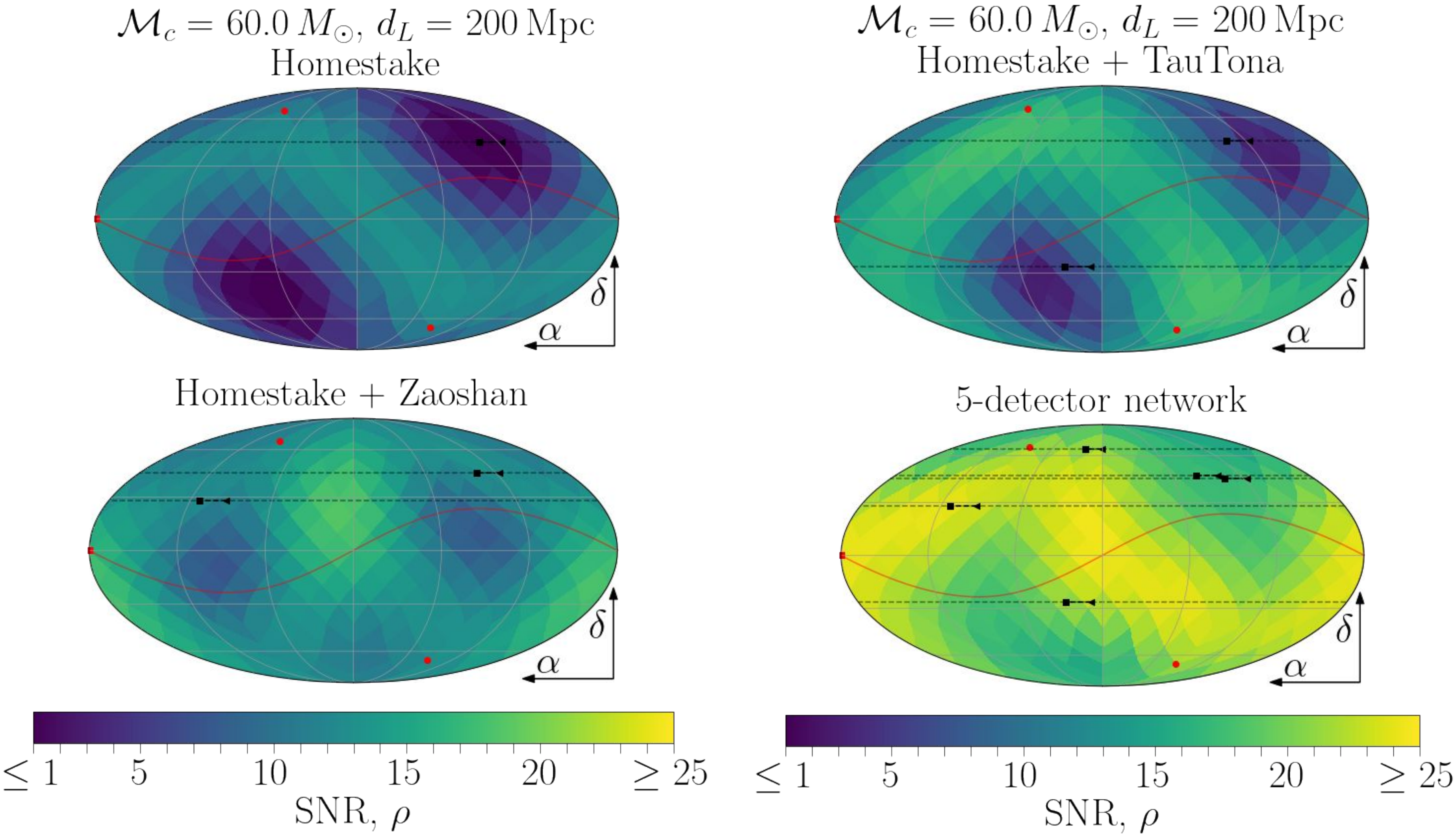

Terrestrial detectors. SNR in skymap

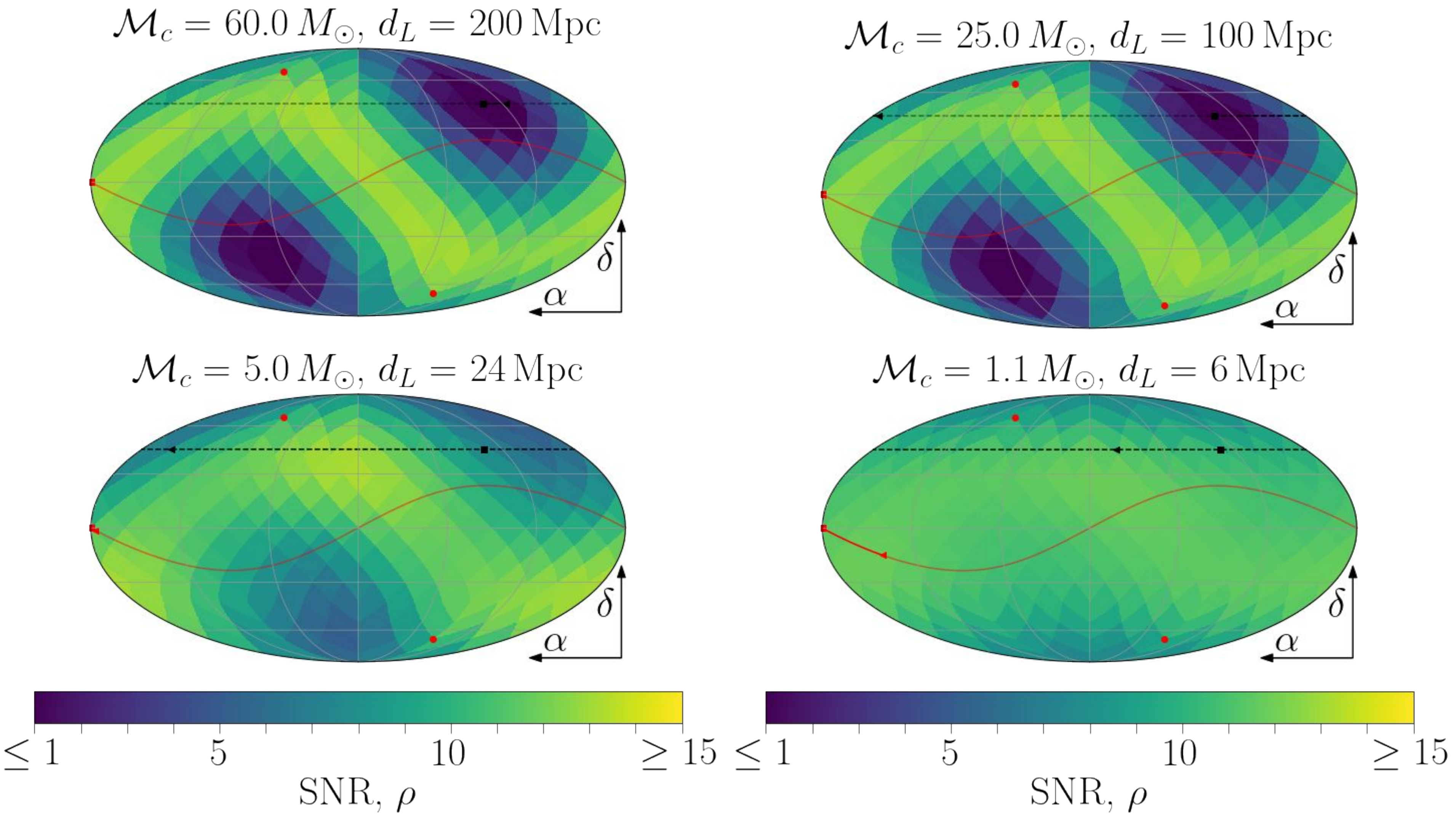

Space detector. SNR in skymap

Compare orbits:

Parallel to ecliptic | 45° to ecliptic | 90° to ecliptic

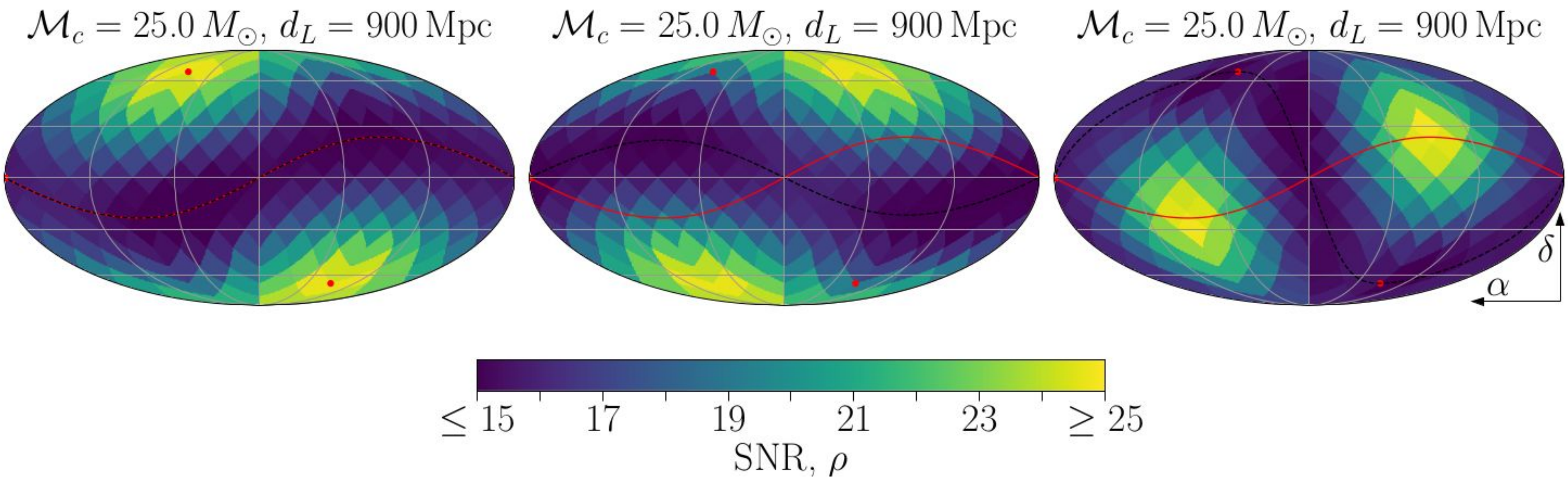

Space detector. SNR in skymap

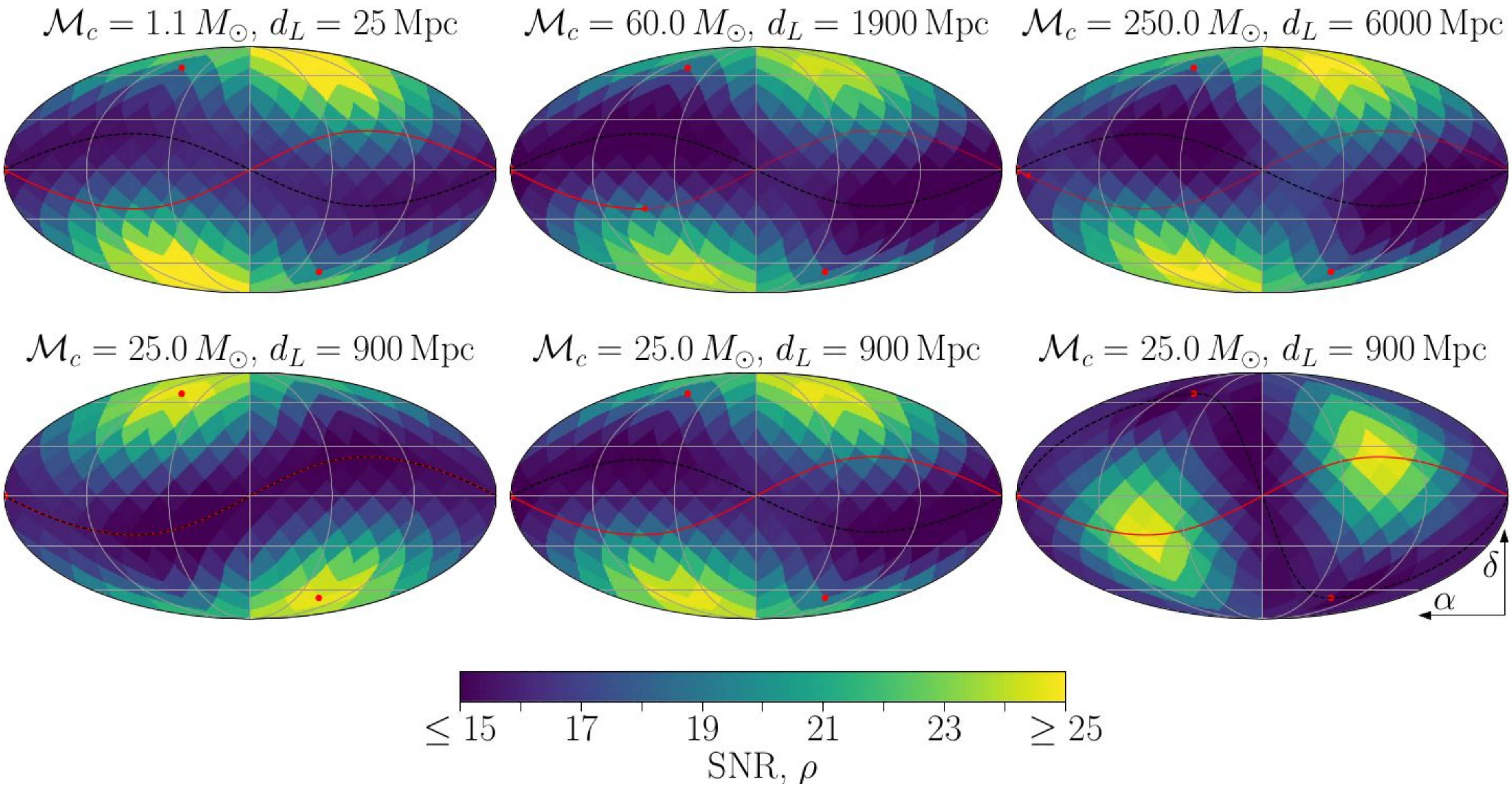

Space detectors. SNR vs $\sigma(d_L)$ in skymap

Parallel to ecliptic | 45° to ecliptic | 90° to ecliptic

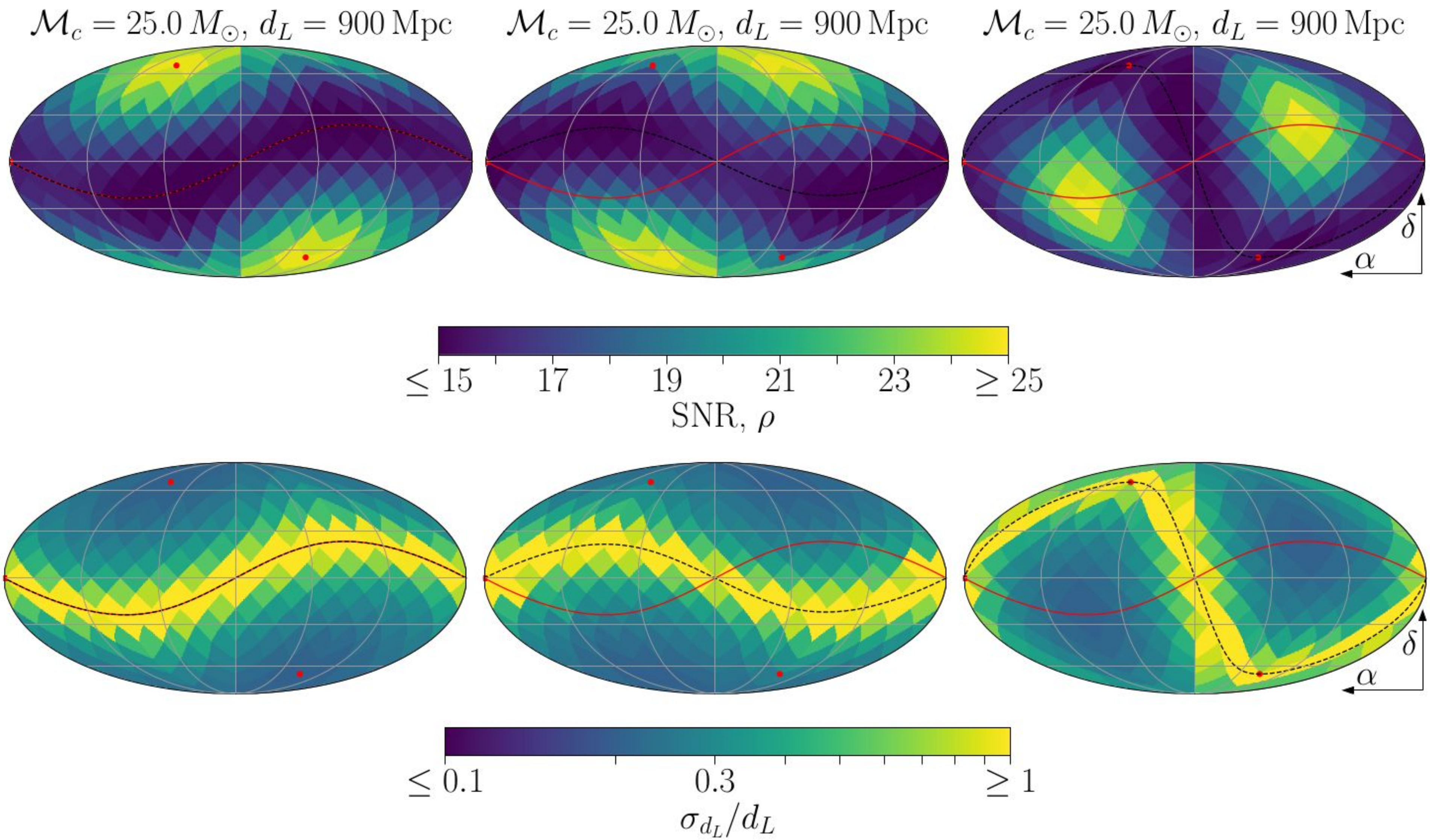

Space detectors. SNR vs $\sigma(\sqrt{\Omega_n})$ in skymap

Parallel to ecliptic | 45° to ecliptic | 90° to ecliptic

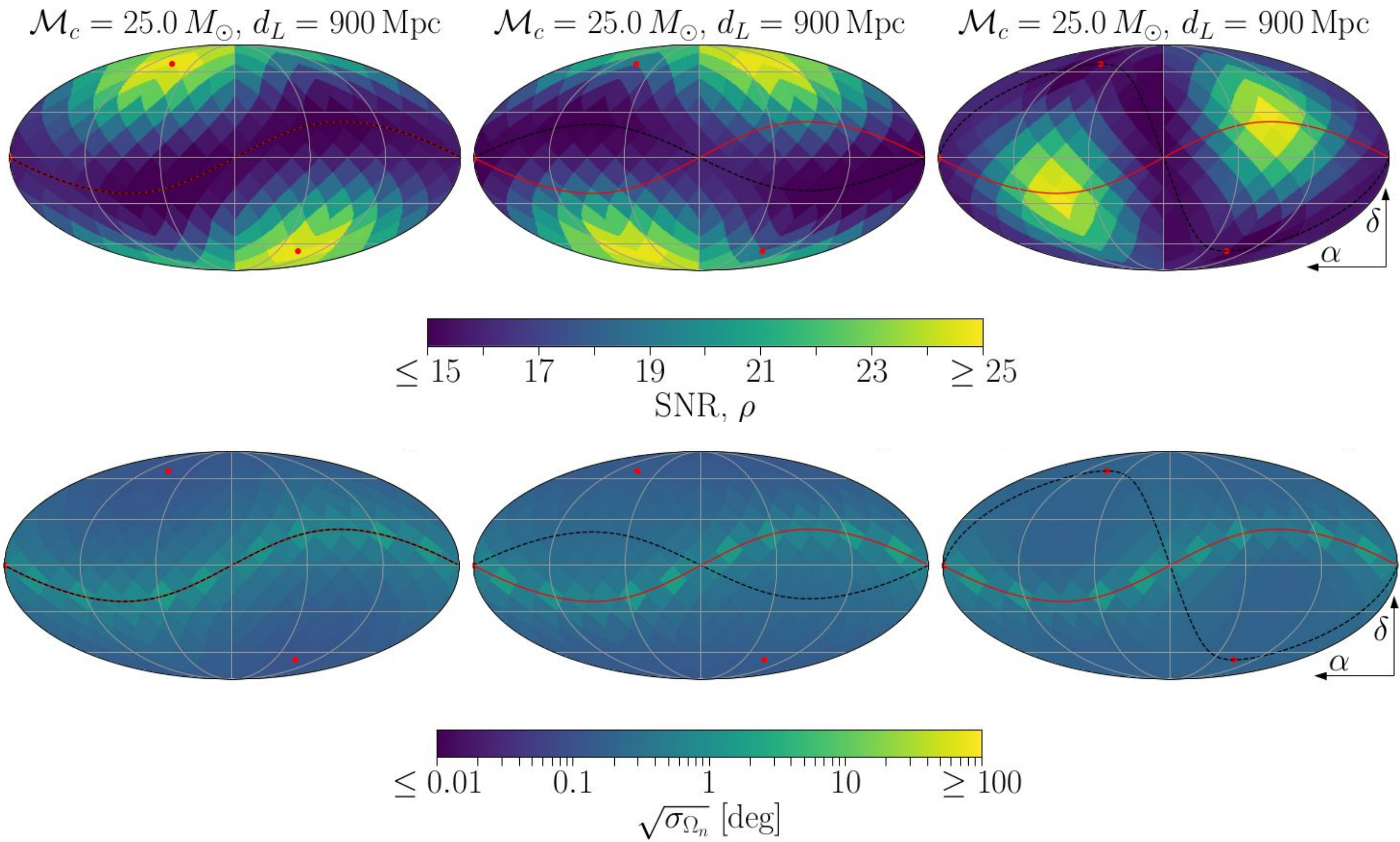

Space detectors. SNR vs $\sigma(d_L)$ in skymap

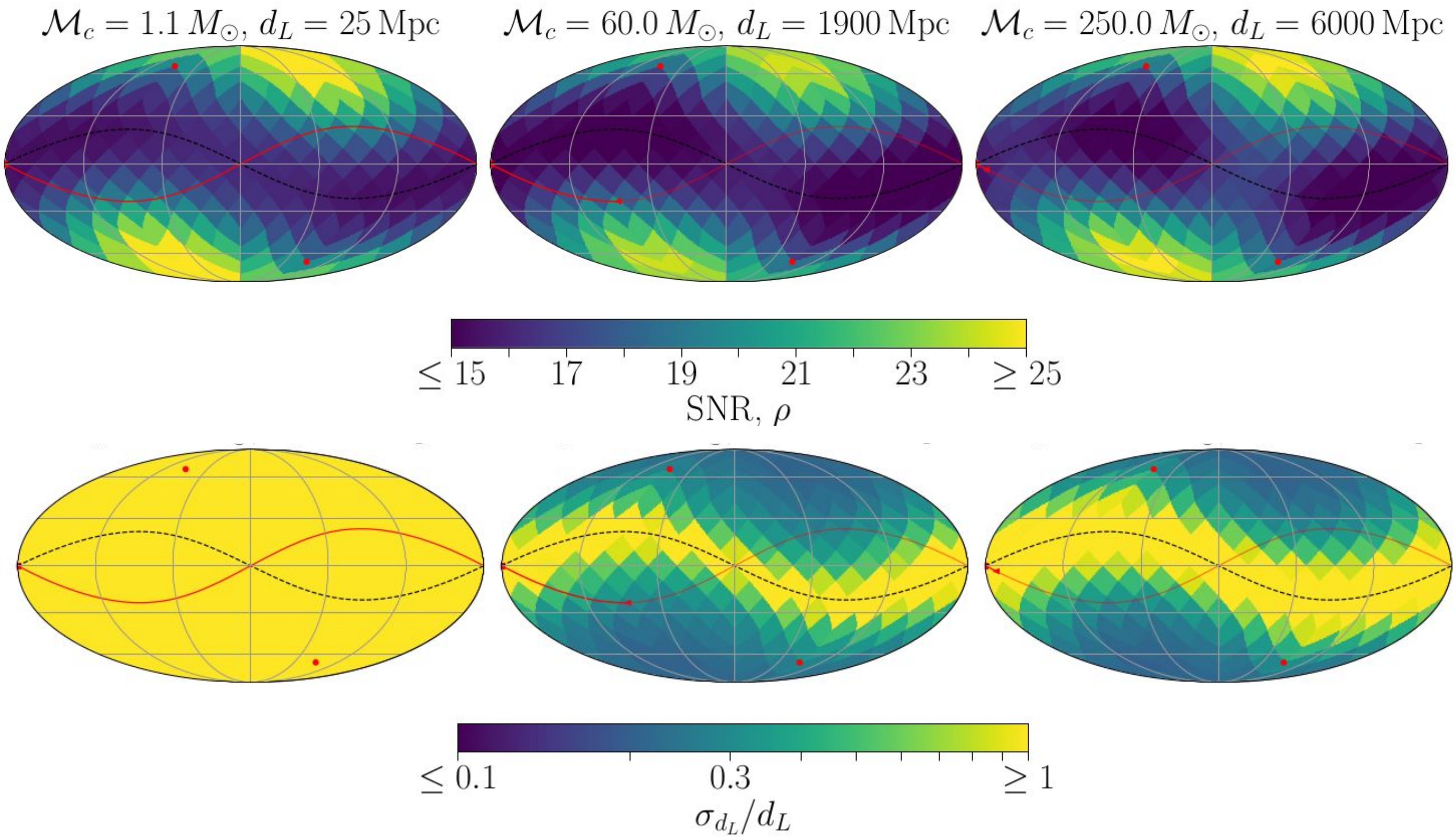

Space detectors. SNR vs $\sigma(\sqrt{\Omega_n})$ in skymap

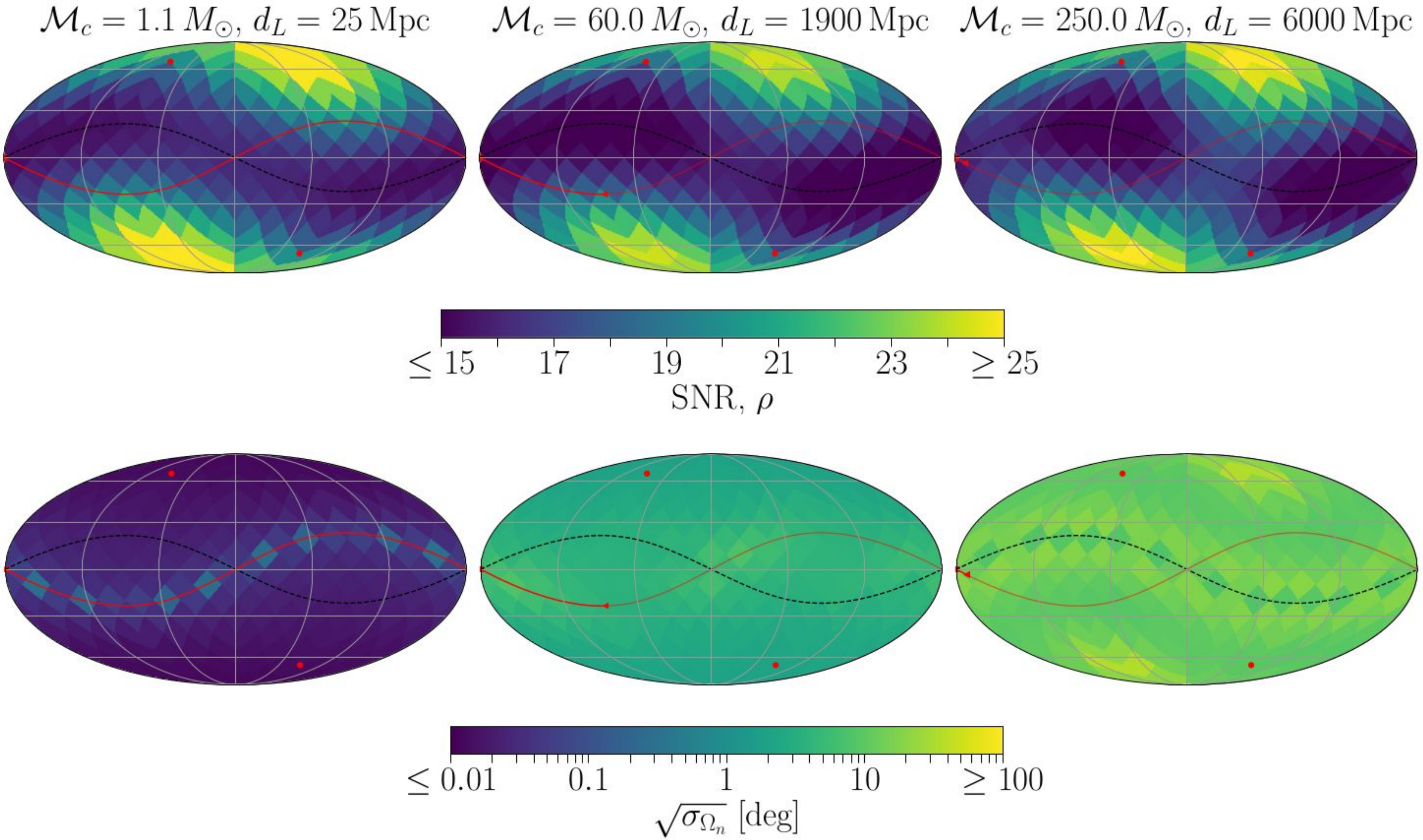

Space detector - the role of Earth

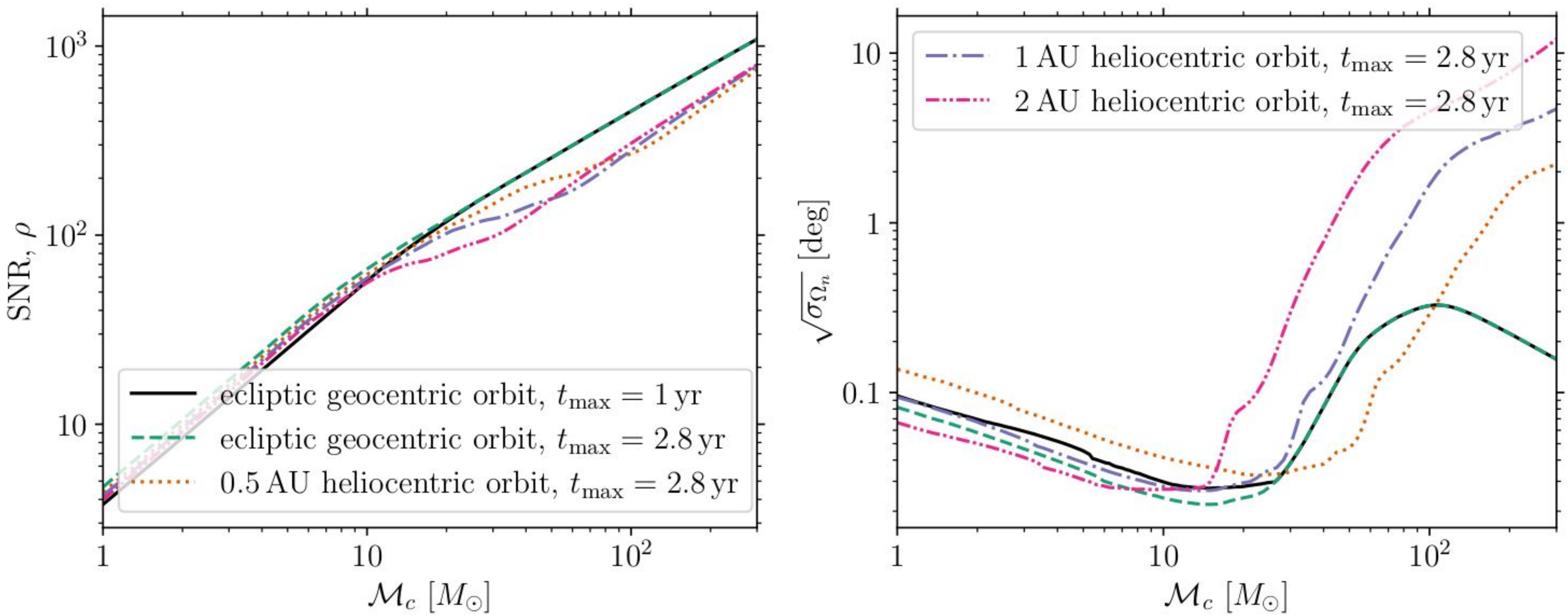

Space-detector. SNR in *L*-space

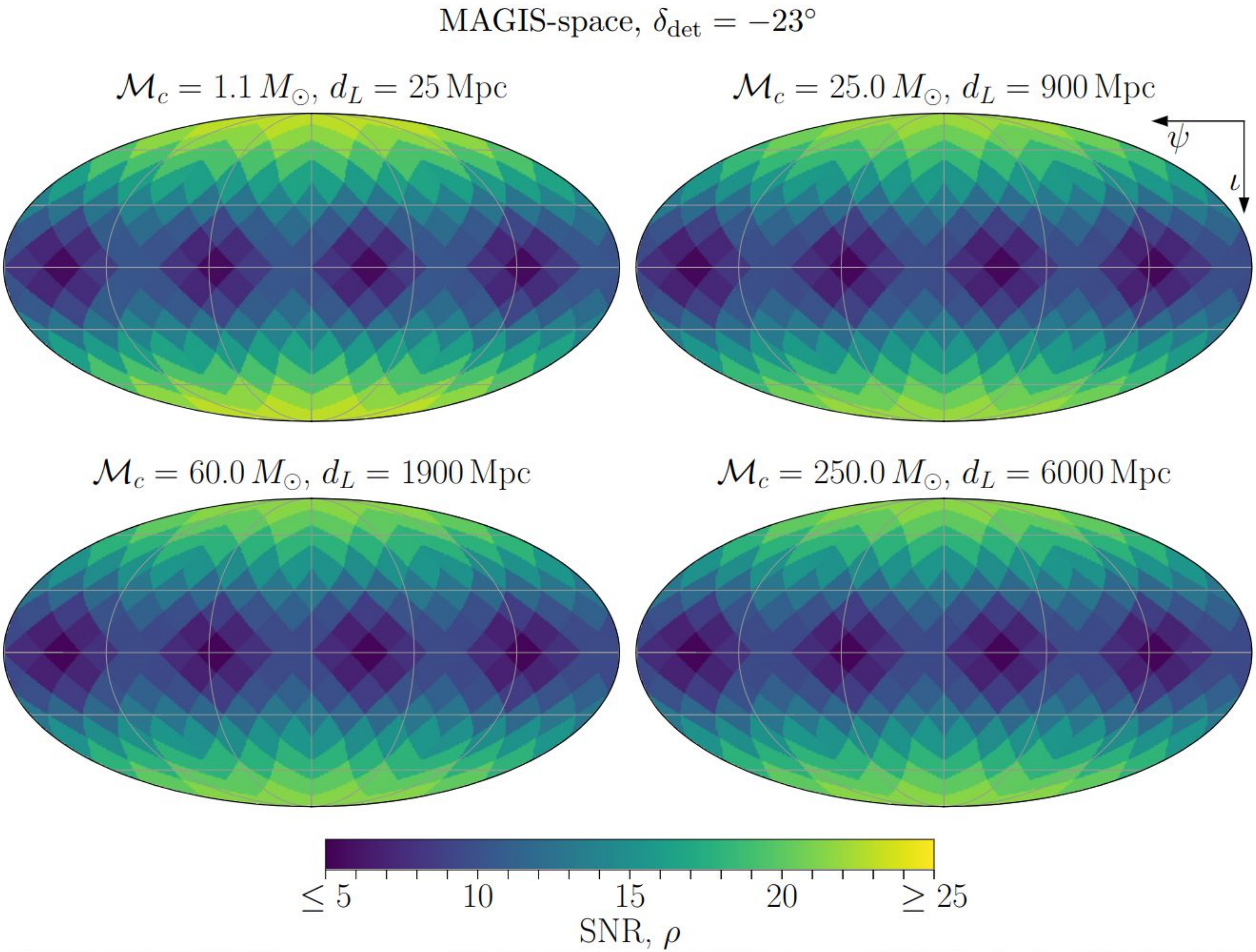

Space-detector. $\sigma(d_L)$ in ***L***-space

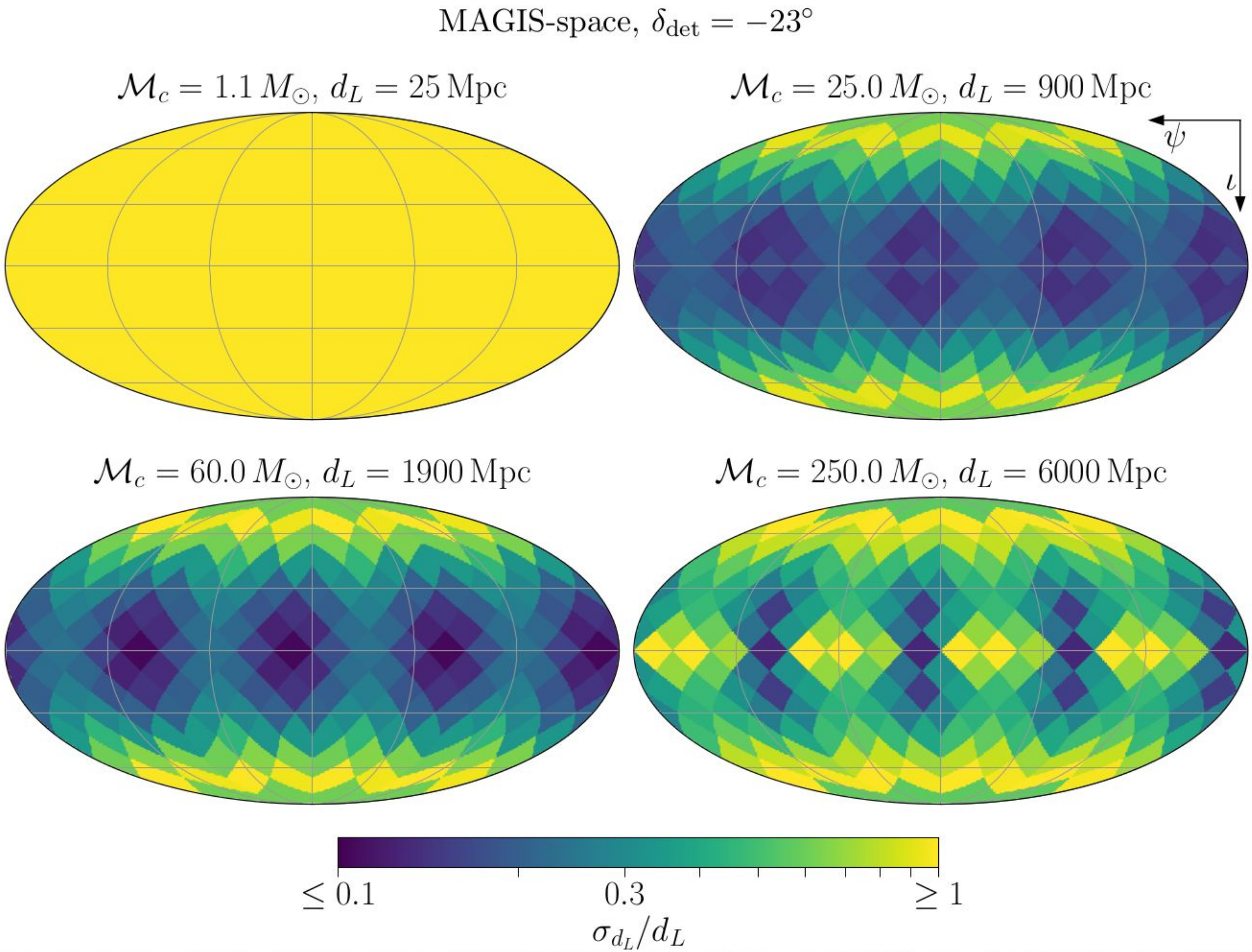

Space-detector. $\sigma(\sqrt{\Omega_n})$ in ***L***-space

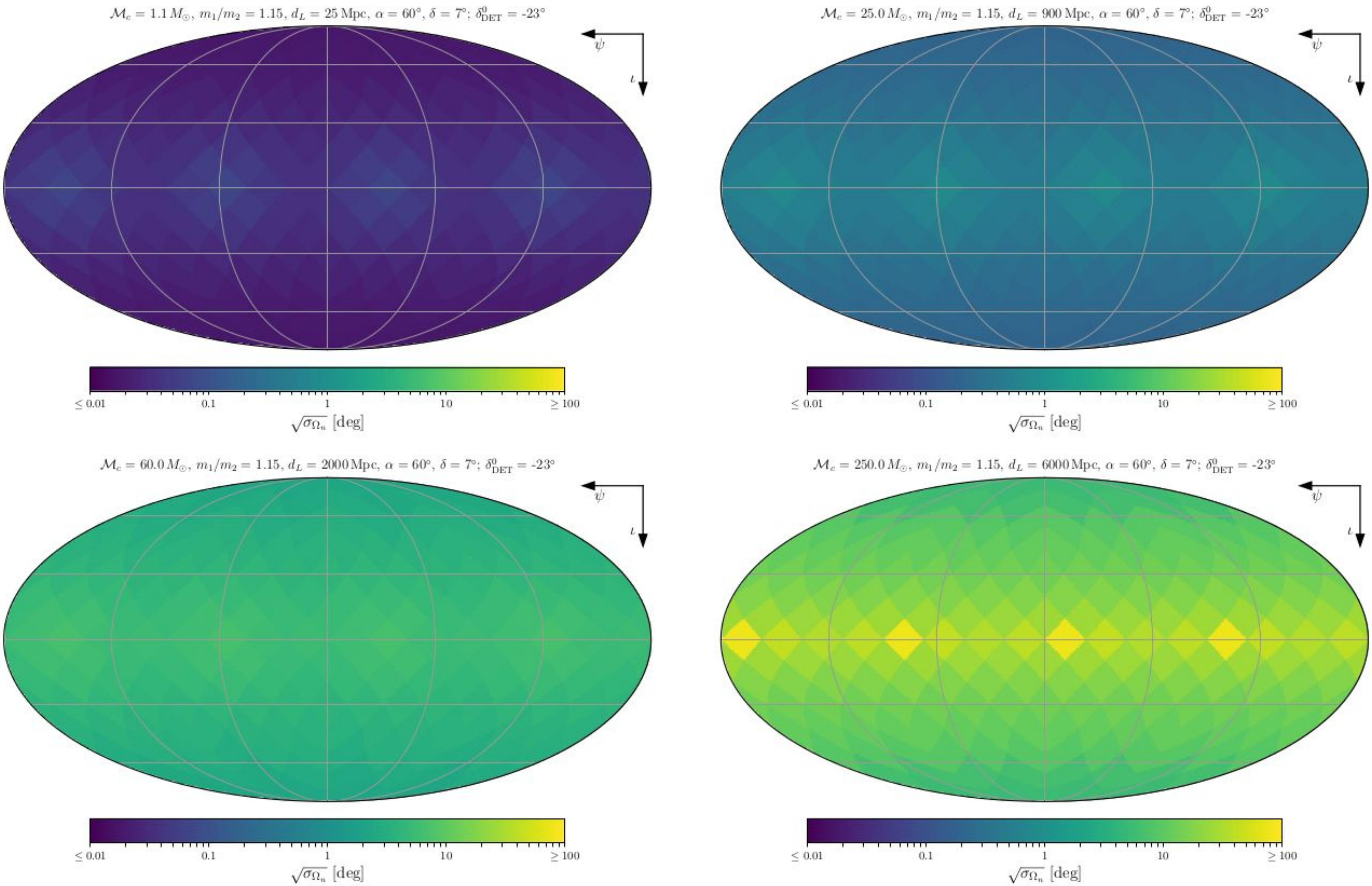

Summary and comments

- Flexible code allows one to explore the capabilities of MAGIS to reconstruct the parameters of GW signals, i.e. to better understand the science case of MAGIS
- Evaluate possible sites for terrestrial MAGIS / different orbits for MAGIS-space
- The mid-band offers unique possibilities for the sky-localization of GW sources
  - Allows for an early warning system for electromagnetic follow-up!
- The mid-band is quite poor at measuring the luminosity distance
  - Combine with terrestrial laser-interferometers?

ICRS: Heliocentric equatorial coordinate system